CLEAN REVISION

Modelling and Identification of Fatigue Load Spectra: Application in the Automotive Industry

E. Bellec[1,2], M.L. Facchinetti[1], C. Doudard[2], S. Calloch[2], S. Moyne[2], M.P. Silvestri[1,2]

[1] Groupe PSA, Chassis System Engineering, Voujeaucourt, France
[2] ENSTA Bretagne, IRDL – UMR CNRS 6027, Brest, France

Abstract

This paper is focused on variable amplitude loading spectra applied in the automotive industry, more specifically for the chassis system parts with respect to high cycle fatigue design. A first analytical model referred to as *Heuler's model* is considered. It is of the simplest use, with one parameter to be identified. A whole identification process, based on road measurement realized on carmaker's proving ground with instrumented vehicles, is developed and discussed. Once the model is identified, the cycles influence on damage production is also investigated. In the light of the obtained results with this model, a second one, noted *modified Heuler's model,* is introduced and investigated. This model, similar to the first, requires the identification of two parameters. Once again, the whole model identification process is applied, and the lifetime accuracy is assessed. A new tool is presented, enabling the visualisation on the loading spectrum representation of the most and less damaging cycles. Hence, a methodology is set to legitimize a gate implementation when studying a variable amplitude loading spectrum.

Keywords: Load spectrum, automotive chassis system, analytical model, parameter identification

1 Introduction

This paper is an extended version of that reported in [1]. The use of Variable Amplitude Loading (VAL) spectra for structure life assessment has met a growing interest among numerous fields since the end of the 20th century ([2], [3], [4], [5]). As outlined in [2], these spectra can be defined from representative load-time measurements (one flight sequence for an overseas passenger aircraft, one-year operation of an offshore platform) or from pre-defined standards (sequences of specific cornering or deceleration for a passenger car). Numerous recommendations exist in the literature ([2], [5], [6], [7], [8], [9]) to set up a circumstance-relevant load case spectrum. Once the representative spectrum is defined, it is applied several times during experiments or numerical simulations until a structure failure appears (e.g. from incipient material crack to definitive integrity loss).

Taking a closer look to the automotive industry, carmakers do not share a standard, nor homologation protocol when it comes to fatigue design. Every firm is free to draft its own fatigue assessment methodology using its own specific proving grounds and relevant load cases. The imperative is to ensure the vehicle security**,** parts integrity and durability and every carmaker must implement a reliable self-certification process. Regarding the fast-changing market, technical cooperation is now an asset. Hence, it is of general interest to share and compare different existing frameworks.

As highlighted in Table 1, many field-specific variable load-time histories have been determined since the 1970's. Through their publications ([10], [11], [12], [13]), P. Heuler & al. describe the various spectrum design steps respecting every physical specificity. As far as the automotive industry is involved, since the 1990's, at least two established variable loading spectra families draw attention regarding fatigue design. The first one, named CAR Loading Standard (CARLOS), gathers reference spectra regarding loads (uniaxial and multiaxial considerations) on suspension parts, powertrain components and car trailer coupling. These spectra are mainly used in the German carmaking industry as fatigue design references. The second proposal is named STAndardized Multiaxial Simulation (STAMAS) ([14], [15]). The vehicle life situations are classified regarding the road condition, and the manoeuvers performed (braking, cornering). This approach has been recently applied to the fatigue strength assessment of chassis system components of a city car [16], nevertheless it is not of wide knowledge, nor application.

These two spectra families are standardised time-loading sequences. To fast forward the fatigue design process and ease the comparison of spectra, VAL spectra should be easily customized depending on the vehicle, the road condition, the driving situation. This study is focused on an analytical spectrum model, based on Road Load Data (RLD) measured both from vehicles operating on the manufacturer proving ground and by real customers on daily usage. Both material and structure design of automotive safety parts vary accordingly to the vehicle of interest. As not to confine oneself to studying a specific safety part, a choice is made in this article to design an analytical model based on the loads measured at the entry point of the chassis system, i.e. the wheel. The scope of this study is high cycle fatigue design ([17], [18]) (i.e. without any yield phenomena) under uniaxial load. The load spectrum design process is illustrated in Figure 1. Regarding measurements performed on the manufacturer proving-ground, the vehicle wheels are equipped with standard force transducers with a 1000 Hz data-acquisition frequency. The measured spectrum usually arises from the concatenation of several vehicle specific manoeuvers and road conditions from the manufacturer proving ground. The sequence of operations is defined by the manufacturer, based on customer feedback ([2], [5]). Each manoeuver is multiplied by a specific

number of times to obtain a representative loading of an ordinary vehicle usage. The spectrum detailed manoeuver composition remains at the manufacturer discretion. The identified model is deemed reliable if its induced damage is equivalent to the one generated by the RLD measurement [19].

Table 1: European standardized sequences and load-time histories ([10])

Name	**Purpose**	**Structure detail**	**Description of load history**	**Load channels[1)]**	**Block size (Cycles)[2)]**	**Equiv. usage**	**No. of load level**	**Year/ ref[3)]**
CARLOS	Car loading standard (3 uniaxial sequences)	Vertical (ve), lateral (la), longitude (lo), forces on front suspension parts	Random with occasional fluctuations of mean stress, mixture of 5 road types, R = -0.18 (ve), -0.64 (la), -1.6 (lo)	1	ve: 136,000 la: 95,200 lo: 84,000	40,000 km	≤ 64	1990/ [20]
CARLOS multi	Car loading standard (multiaxial)	4-channel load components for front suspension parts	Time histories, sample frequency 0.005 sec, correlation functions between load components based on guide functions	4	Similar to CARLOS uniaxial	40,000km	/	1994/ [21]
GAUSSIAN	General purpose random sequence	Narrow-band to wide-band random (3 levels of irregularity, I)	I=0.99 - no mean stress fluctuation. I= 0.70- minor mean str. fluctuation. I= 0.33- considerable mean str. fluct.	1	$1.0*10^6$ $1.4*10^6$ $3.3*10^6$	-	20	1974/ [22]
TWIST	Transport aircraft wing root	Wing root bending moment	Constant positive mean stress. For gust loads, ground-air-ground cycles (GAG) = underloads	1	402,000	4,000 flights	20	1973/ [23]
WAWESTA	Stell mill drive	Drive train components	Sequence of 10.000 milling runs	1	28,200	1 month	23	1990/ [24]

[1)]No of load components or additional variables (time, temperature etc.); [2)] approx. [3)] partly the references do not cite the original report(s), but those available to the public

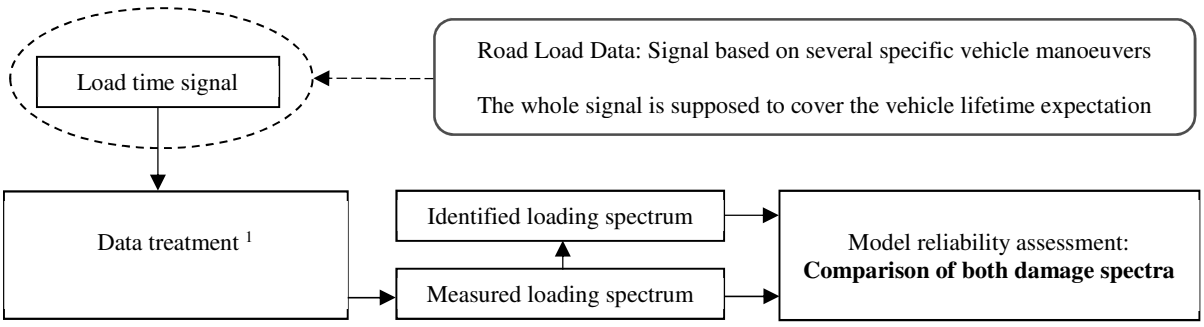

Figure 1: Load spectrum design steps and model reliability criterion

The first part of this article highlights the approaches found in the literature to represent a structure life assessment under variable amplitude loading (section 2.1). The theoretical assumptions and damage calculation methods are depicted (section 2.2). Throughout the article, considering the fatigue assumptions made, the most impacting amplitudes are investigated (sections 2.3 & 2.4). The RLD measurement is set as a reference. To represent the whole RLD complexity and find a standard model, the attention is drawn to an analytical loading spectrum formula (section 3). The lifetime model estimate accuracy is then discussed. Regarding the achieved results, a slight modification to this formula is suggested. Once again, the model theoretical behaviour and damage-induced accuracy is investigated (sections 4.1 & 4.2). A methodology, based on theoretical fatigue-related tools, is finally proposed to find and remove from spectra either the least or non-damaging cycles (section 4.3).

[1]: The rainflow counting method is used all along this study to count the number of cycles per loading amplitude range. Other counting method exist such as range-pair, level-crossing, …

Nomenclature
Notation list

$\boldsymbol{S}$	Loading amplitude vector
$\boldsymbol{S_i}$	Loading amplitude numbered i. The amplitudes are classified in descending order
$\boldsymbol{S_{max}}$	Maximum amplitude of the loading spectrum
$\boldsymbol{N}$	Number of cycles to failure (valid for constant and variable amplitude loadings)
$\boldsymbol{N_i}$	Number of cycles to failure corresponding to the constant amplitude loading S_i
$\boldsymbol{H}$	Cumulative occurrences vector
$\boldsymbol{H_i}$	Cumulative occurrences, from S_{max} to S_i,
$\boldsymbol{H_0}$	Cumulative occurrences, spectrum overall length
$\boldsymbol{n}$	Number of cycles performed per amplitude block for a given loading spectrum
$\boldsymbol{n_i}$	Number of cycles performed at a given amplitude range S_i
$\boldsymbol{b}$	Basquin slope, material parameter
$\boldsymbol{B}$	Basquin constant, material parameter
$\boldsymbol{SSF}$	Spectrum shape factor
$\boldsymbol{k}$	Gassner slope, material parameter (= b, Basquin parameter)
$\boldsymbol{d}$	Damage vector
$\boldsymbol{d_i}$	Damage induced per amplitude range, for a given loading spectrum
$\boldsymbol{D_{tot}}$	Total damage induced by the overall spectrum
$\boldsymbol{D_{cu}}$	Cumulative damage vector
$\boldsymbol{\nu}$	Model shape exponent parameter (applied in Heuler's model and modified Heuler's model)
$\boldsymbol{\alpha}$	Model starting point parameter (applied in modified Heuler's model)

2 Representation and damage assessment of recorded load spectra

This section aims to set the study theoretical framework. The usual methodologies applied to assess fatigue lifetime are depicted, at first under constant loading, then under variable amplitude loading (section 2.1). Loadings studied in this article are measured at the wheel. Even during the most critical manoeuvers, in the framework of normal usage, the maximum stress undergone is expected far from the vehicle parts yield stresses. The RLD spectrum and its damage are represented (section 2.2). Even if very low amplitude cycles are not expected to cause relevant fatigue damage, no cycle omission is applied a priori. Only basic temporal noise filtering is considered. No endurance limit is considered. The damage calculation, specific to this study, is based on a Basquin-like formulation [25]. Hence, the impact of the Basquin slope value is investigated (section 2.3) and an analytical tool named "iso-damaging curve" is used to detect the most impacting amplitude range from a given loading spectrum (section 2.4).

2.1 Variable amplitude framework

Usually, fatigue life assessment is represented by means of Wöhler curve [26] (Figure 2) combining, for a given material (and process), the number of cycles until a given failure criterion (e.g. crack initiation), "N_i", to the loading amplitude "S_i". This curve is built up thanks to experiments and is expected to be applied for constant amplitude loadings.

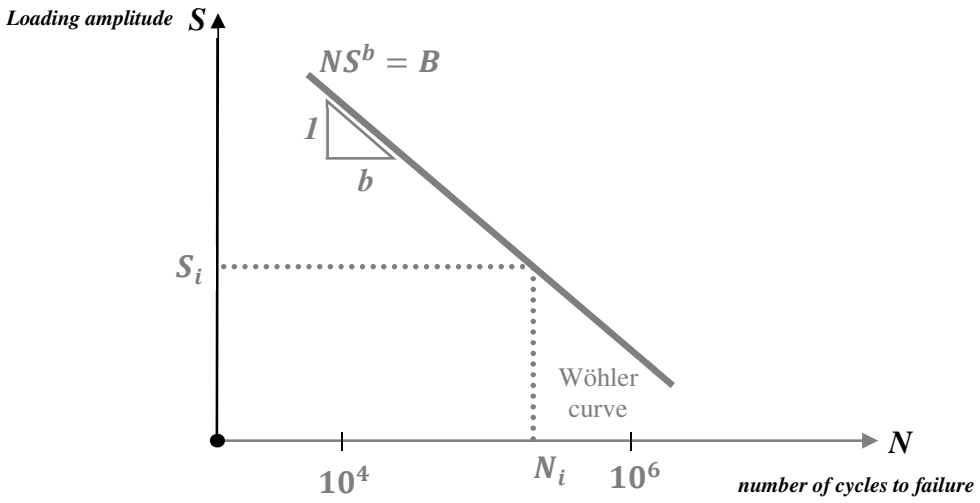

Figure 2: Standard high cycle fatigue framework for constant amplitude loading, Wöhler curve

As depicted in Figure 2, the Wöhler curve, sketched in a logarithmic frame, is like a straight line. It is a legitimate interpretation especially illustrated by metals between 10^4 and 10^6 loading cycles. The relationship between S and N is then described by the following Basquin formula

$$NS^b = B. \quad \textbf{(1)}$$

Both parameters "b" (>1), the Basquin slope and "B" (>>1), the Basquin constant, are material dependent to be identified. It has been reported through literature reviews [27], that "b" does not only vary accordingly to the material but also to the process, i.e. the assembly procedure. For instance, the Basquin slope, "b" is expected to range from 2 to characterize a welded joint (minimum found for any application), to 8 and even more for a steel plate. For automotive applications, please consider that if the Basquin slope is assumed to be bigger than 8**,** high cycle fatigue requirements are not expected to be relevant anymore. Considering "B" fixed, the more "b" increases, the more higher loading amplitudes are damage producing.

As the Wöhler curve is applied for constant amplitude loading, in 1939, E. Gassner [28] presented a new approach to characterize structure lifetime assessment under VAL. The main innovation is not to represent the loading spectrum thanks to an S-n curve but replacing actual cycles "n_i" (i representing the amplitude range) by cumulative occurrences noted "H_i" (Figure 3). They are calculated using the following relationship

$$H_i = \sum_{k=1}^{i} n_k. \quad \textbf{(2)}$$

The maximum amplitude is set to " S_1". At this amplitude the number of cycles is noted "$n_1 = H_1$". At the spectrum lowest amplitude, the spectrum overall length is noted " H_0". The first loading spectrum designed by Gassner was built for the aeronautic industry. It is inspired from a gaussian-like curve divided into 8 amplitude blocks. Its simplicity was imposed by the experimental limitations set at that time.

Nowadays, much more complex and realistic loading spectra can be reproduced on test benches or computed by numerical simulations. Once the maximal amplitude "S_{max}", the overall length " H_0", and the shape are defined, the spectrum can be applied several times to the structure until failure. Hence, the lifetime can be assessed thanks to cumulative occurrences, regarding the number of times the overall loading spectrum has been applied. To be accepted as an elementary spectrum, its overall length should be one order of magnitude under the lifetime expected. E. Gassner suggested a Wöhler-like curve to represent structures lifetime under a given variable loading spectrum. Both curves can be represented thanks to the number of cycles up to failure "N". The main difference lies in the amplitude dependency. The regular Wöhler curve is depicted thanks to the constant amplitude loading "S". Once the shape of the spectrum is set, the Gassner one is "S_{max}" dependent. Thus, the overall lifetime has been reported to the "$logS_{max} - logN$" curve. The failure curve equation is another Basquin-like formula noted

$$NS_{max}^{k} = K. \quad (3)$$

Once again, the ("*k*", "*K*") are material/process parameters to be identified. Previous researches show the equality between "*k*" and "*b*" values from the Gassner and the Basquin formula. This has been mathematically proven if the Palmgren-Miner damage accumulation law is applied: "*k* = *b*". Actually, as both slopes' values are supposed to represent the same material physical behaviour, it is of common sense to consider them equal.

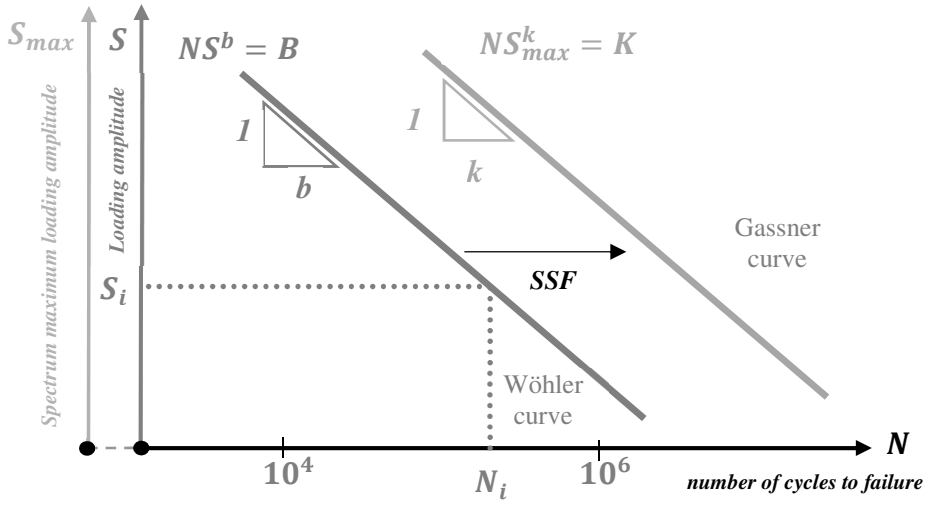

Figure 3: Standard high cycle fatigue frameworks, Wöhler and Gassner curves

Comparing both failure curves on Figure 3, the Gassner one seems to quantify a longer lifetime than the Wöhler one. Even if the slope value is the same ("*b = k"*), the value of "*K"* and "*B"* are different. The impression of longer lifetime is a graphical mirage. Both curves are not represented in the same frame even if they are similar: ("*S", "N"*) for the Wöhler curve and ("S_{max}*", "N"*) for the Gassner one. To shift from one representation to the other, P.Heuler (6,7) defined the following coefficient, named Spectrum Shape Factor (SSF),

$$SSF = \log\left(\frac{\sum n_i}{\sum n_i (S_i/S_{max})^b}\right). \quad (4)$$

It essentially depends on the spectrum shape and the Basquin slope. If the VAL turns out to be a constant one, equal to "S_{max}", the SSF would be equal to 0 and both curves would match (reference frames end up the same one). This factor is always definite positive as "*b"* and "S_i/S_{max}" are respectively greater and lower than 1. The factor is lower than the unit value (<1) for spectra with many large and few small cycles. On the contrary, its value rises when the number of cycles at the highest amplitudes is preeminent compared to the lowest ones. Heuler investigated the SSF coefficient based on Gassner's first VAL spectrum. The SSF value is about 2.5. The Gassner curve would be shifted from the Wöhler curve at least of two orders of magnitude on the right. Heuler investigated

also several VAL spectra developed in the industry and found the SSF coefficient, reported in Table 2 (using "$b = 5$" as the Basquin slope value).

Table 2: European standardized sequences corresponding SSF values (extracted from [10])

Name	SSF
CARLOS	*2.66*
CARLOS multi	*2.70*
GAUSSIAN	*2.32*
TWIST	*3.09*
WAWESTA	*1.97*

An SSF value may correspond to several loading spectra. Hence, knowing only the maximum loading amplitude and the spectrum corresponding SSF value is not enough to depict all the spectrum loading complexity. It is therefore required to use the entire loading spectrum to identify a reliable loading model for fatigue design.

2.2 Spectrum representation and damage-like tool formulation

Before using any of the fatigue design frameworks introduced previously, the measured spectrum coming from RLD is displayed in Figure 4. (A choice is made by the authors regarding the spectrum display reference frame: ("*S-n*") or ("*S-H*"). The reader must keep in mind that the RLD introduced is representative of a car loading experienced in real life situation.

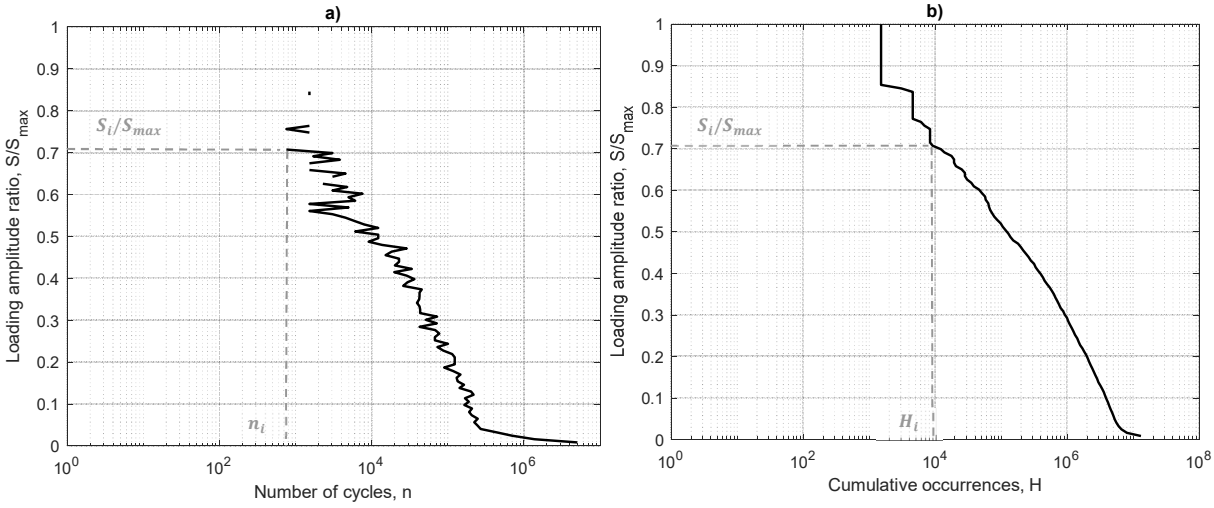

Figure 4: VAL coming from RLD, represented via effective cycles (a) and cumulative occurrences (b)

Representing the loading spectra thanks to the loading amplitude ratio "S_i/S_{max}" eases the comparison between different RLD patterns e.g. impact of the vehicle tested, the executed manoeuvers, the road conditions …

Regarding the abscissa, the first graph, Figure 4 a) turns out to be quite irregular and thus tough to be described via an analytical model. On the contrary, the second graph, representing the same loading spectrum as the first one but using cumulative occurrences, is smoother and eases the identification process. The other advantage of cumulative occurrences representation is the independency towards the amplitude scale size.

As expected, there are much more cycles at the lowest amplitudes than at the highest ones. The spectrum identification from 0.5 to 0.1 seems to be easily achievable. Nevertheless, there are some step-like irregularities at the highest amplitudes that might be difficult to represent. Thus, both frameworks have some shortcomings in order to seek for a simple analytical model to fit the overall spectrum shape.

As these loading spectra are meant to design a chassis system under high cycle fatigue, it is proposed to compare the damage induced by the RLD and the one coming from the identified model to decide which analytical loading model is best fitting. The damage calculation formula used in this study is not based on the cumulative occurrences ("*H*") but on the effective number of cycles ("*n*") per amplitude. By using the Palmgren-Miner's rule ([29], [30]), the overall damage induced by the spectrum, "D_{tot}", is then given by

$$D_{tot} = \sum d_i = \sum n_i/N_i = \sum n_i S_i^b/B. \qquad \textbf{(5)}$$

For each amplitude range "S_i", the damage "d_i" is equal to the number of cycles executed "n_i", divided by the lifetime at the same amplitude "N_i". Assuming that the Basquin formula is used to assess the structure lifetime under constant amplitude loading, "N_i" can be replaced by "B/S_i^b". The "B" value is a material parameter to define. In the study instance, the loading spectrum is measured at the vehicle wheel. Thus, the damage calculation is not based on any specific chassis part material. To ease the comparison between RLDs performed on different vehicles, "B" is fixed to "$S_{\max}^b$", (this normalization helps to notice if the damage spectrum shape differs significantly). The damage equation per amplitude block is noted

$$d_i = n_i(S_i/S_{max})^b. \qquad \textbf{(6)}$$

This formula has no proper physical meaning. It just enables to link the amplitude ratio to the damage and compare the different damage spectra coming from several measurements together. Based on this damage-like formula with a Basquin slope value of 5, the damage induced by the RLD presented in Figure 4 is calculated.

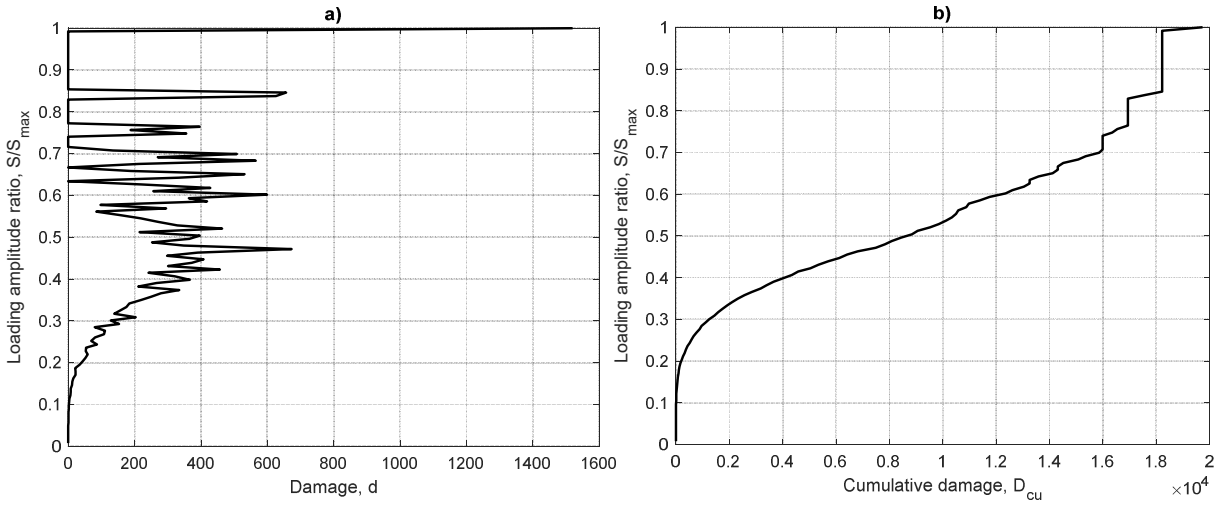

Figure 5: Damage (a) and cumulative damage (b) induced by RLD (b=5)

The Figure 5 highlights the impact of the highest amplitudes on the lifetime (from 0.8 to 1 for "S/S_{max}"). The Figure 5 b) represents the cumulative damage, "D_{cu}", according to the spectrum loading amplitude ratio. The cumulative damage is increasing with the loading ratio to finally reach the overall damage "D_{tot}" at the highest amplitude "$S_i = S_{max}$".

This damage representation illustrates some useful information. The maximum amplitude loading block (refer to Figure 5 b) upper right corner) induces almost 10% of the overall damage with only 0.01% of the overall spectrum length (referring to the number of cycles in the spectrum). The other way around, at the lowest amplitude, 10% of the overall damage is induced by 98% of the spectrum overall length, corresponding to an amplitude ratio from 0 up to 0.35. Definitively, working with cumulative damage ("$D_{cu} = 0$" for "$S = 0$" and "$D_{cu} = D_{tot}$" for "$S = S_{max}$") instead of regular damage is the opportunity to eliminate a majority of the fluctuations, the amplitude scale definition dependency, and to analyze at a glance the cumulative damage curve slope and the final value, respectively.

2.3 Material parameters impact on the damage spectrum shape

This chapter reports the damage spectrum shape, based on the damage calculation formula, for several Basquin slope values. As the Basquin constant "$B = S_{max}^b$" is "b" dependent, it is senseless to compare the cumulative damage curves one with another without damage normalization. The cumulative damage curves shape should be compared assuming each curve is normalized respectively by its overall damage induced. The Figure 6 highlights three normalized cumulative damage curves, all calculated from the RLD, with different Basquin slope values "b".

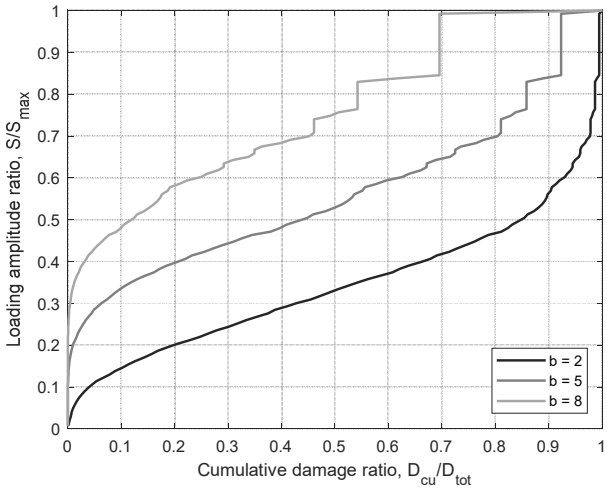

Figure 6: Normalized cumulative damage induced by RLD, with different Basquin slope values

The higher is b, the highest amplitudes impact on damage calculation is more significant. For information, regarding these specific loading sequences:

- "b = 2". 98% of the spectrum length (Number of cycles n from "$S_i/S_{max} = 0$ to 0.4") induces 65% of the overall damage at the lowest amplitude.
- "b = 5". 98% of the spectrum length induces 20% of the overall damage. 0.01% of the spectrum length, belonging to the highest amplitude induces almost 10% of the overall damage.
- "b = 8". 98% of the spectrum length induces 3% of the overall damage. 0.01% of the spectrum length, belonging to the highest amplitude induces 30% of the overall damage.

Considering the future model identification process, this aside reveals that the more "b" increases, the more the model accuracy should be focused on higher amplitudes. If there is no contrary specification, a Basquin slope value "b = 5" (according to automotive literature for average quality components) is considered in the rest of this study.

2.4 Amplitude of interest using iso-damaging tool

The previous section enables to find the most damaging amplitude (depending on the Basquin slope value) by looking at the cumulative damage graph. Considering the studied loading spectrum and regardless of the "b" value, all the amplitudes do not participate to the same extent in the damage. This section aims to detect the most damaging amplitudes, directly from the loading spectrum representation using a pragmatic tool: "the iso-damaging" curves.

Iso-damaging curves are supposed to cause the same amount of damage per amplitude range, i.e. a uniform damage through the entire spectra. Hence, they are "b" dependent. The iso-damaging curves presented in

this section are also calculated using the damage formula (6) presented in section 2.2. Once the overall amount of damage induced "D_{tot}" and the number of loading amplitude classes "j" are set, the iso-damaging curve can be derived. The damage for the loading amplitude class "S_i" can be related to "D_{tot}" and "j" by

$$\forall\, i \in [\![1, j]\!]\,, d_i = D_{tot}/j = n_i(S_i/S_{max})^b. \qquad (7)$$

This equation can be reformulated to determine the number of cycles for each loading amplitude class, "n_i", for a given "D_{tot}",

$$n_i = (D_{tot}/j) * (S_i/S_{max})^{-b}. \qquad (8)$$

The lower the cumulative damage curve slope gets (definite positive), the more the corresponding amplitude range is damaging. When the amount of damage per amplitude range is defined, the corresponding number of cycles can be determined. Hence, the corresponding loading spectrum can be displayed (Figure 7). For this study, the size of the amplitude classes is fixed to 50N. (Order of magnitude: 1%, compared to the "S_{max}" measured)

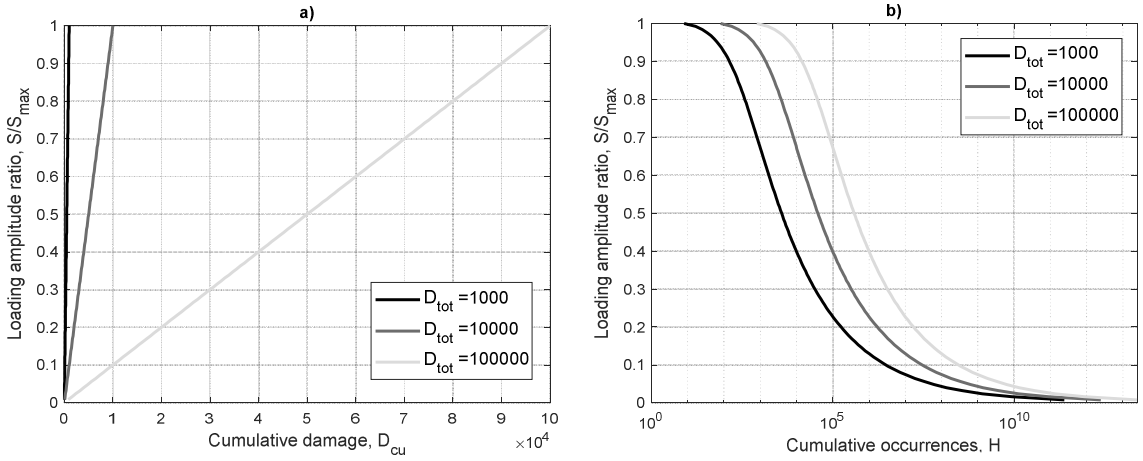

Figure 7: Iso-damaging curves: cumulative damage framework (a) and associated loading spectra (b)

In this study, the iso-damaging curves are used as a tool to compare the damages induced for different amplitude classes from the RLD spectrum. When the RLD curve matches an iso-damaging curve at a certain point, it indicates that the damage induced at this specific amplitude range by the loading spectrum is equal to the one caused by the iso-damaging curve.

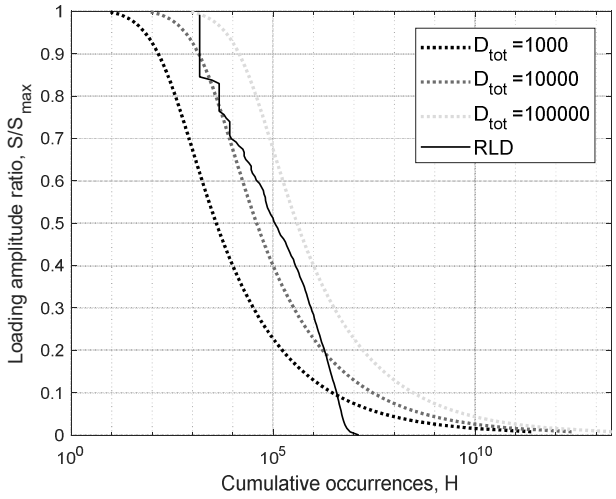

Figure 8: Comparison between the RLD and the iso-damaging curves

Considering the Figure 8, three main observations can be expressed:

- At the highest amplitude, the RLD is as damaging as the "$D_{tot} = 10^5$" curve.
- At the medium amplitudes, the most damaging amplitude ranges are around "$S_i/S_{max} = 0.4$" regarding the RLD spectrum. Still, the loading spectrum induces less damage at these amplitudes than the "$D_{tot} = 10^5$" curve.
- At the lowest amplitudes, "$S_i/S_{max} < 0.2$", the loading spectrum is less damaging than "$D_{tot} = 10^4$". It is even lower than "$D_{tot} = 10^3$" when "$S_i/S_{max} < 0.1$".

Once the damage formula is set, using the iso-damaging tool is of great interest to compare the most and least damaging cycles for a given spectrum shape. These observations highlight that cycles at the lowest amplitudes, even if they compose at least 50% of the overall spectrum length, are 100 times less damaging than cycles at the highest amplitudes. To go further, this tool may be used to legitimize the omission of some non-damaging cycles from the initial spectrum, also known as "gate implementation" process. The gate amplitude corresponds to the amplitude under which no cycles are actually counted into the spectrum.

3 Heuler's model identification

This section aims to present the VAL model formerly proposed by P. Heuler in the literature ([10], [11]). A first theoretical study is provided regarding the different spectra shapes that can be modelled (section 3.1). Then, the model is identified based on the RLD previously introduced and its fatigue life assessment accuracy is evaluated (section 3.2).

3.1 Model formulation and theoretical investigation

The analytical model formula designed by P. Heuler ([10], [11]) is

$$\log(H)\,/\log(H_0) = 1 - (S/S_{max})^{\nu}. \qquad \textbf{(9)}$$

This model seems quite flexible as P. Heuler used it to clarify and compare all the spectra loading shapes considered by Gassner. It is defined based on cumulative occurrences and loading amplitude ratio. The coefficient "ν" is named shape exponent. This one parameter model dependent (considering the parameters responsible for the scaling "H_0" and "S_{max}" are already known) can reproduce several different VAL. The Figure 9 illustrates different spectra shapes according to "ν", with "$H_0 = 10^7$" cycles. As the cumulative occurrences' framework can be tricky to figure out, the graph b) illustrates the same spectra regarding the effective number of cycles. The model can reach a wide variety of behaviours especially at the lowest amplitudes.

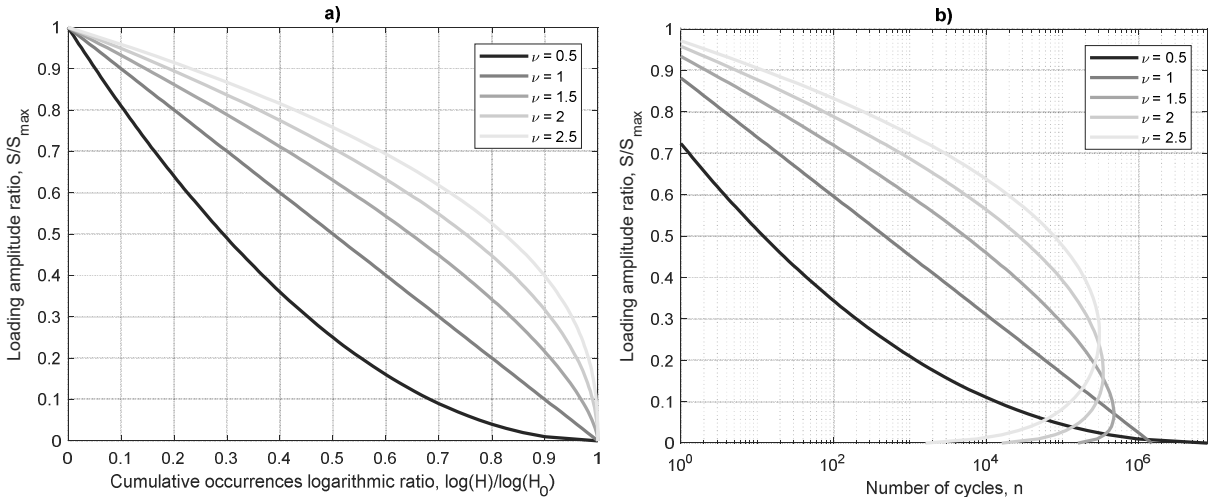

Figure 9: Heuler's model load spectra, via cumulative occurrences (a) and regular number of cycles (b)

Three main spectra behaviours emerge from this model regarding the shape exponent value:

- "ν < 1": much lower number of cycles at the highest amplitudes than at the lowest. "H" is increasing faster while the amplitude is decreasing. These spectra would be considered for soften driving behaviour.
- "ν = 1": linear relationship between the amplitude ratio and the cumulative occurrences ratio.
- "ν > 1": spectra slope is lower at the highest amplitudes than at the lowest. The more the coefficient increases, the more the maximum effective number of cycles is reached at a higher amplitude. These spectra would feat a stiffer driving behaviour.

Table 3, coming from [10], correlates some of the spectra's shape depending on ν to the SSF value introduced in section 2.1.

Table 3: Spectrum shape parameters ν and SSF for typified amplitude spectra (extracted from [10])

Spectrum	ν	SSF	Description
1	∞	0	Constant amplitude loading
2	4	1.46	$\nu > 2$ typical for bridge and crane structures
3	2	2.45	Stationary gaussian random process
4	1	3.77	Typical for road roughness induced loads
5	0.8	4.21	$\nu \leq 1$ typical for wind gusts, wave actions, etc.

Based on P. Heuler's previous work, the shape factor coefficient is expected to sway between 0.5 and 5 to match the various standardized variable load-time histories presented in Table 1.

In the scope of this study, this spectrum model aims to be used for fatigue design. Hence, in the same vein of section 2.2, the damage spectra coming from Heuler's model is investigated. As the shape factor impacts the overall damage value, only the normalized cumulative damage curves are inspected in Figure 10.

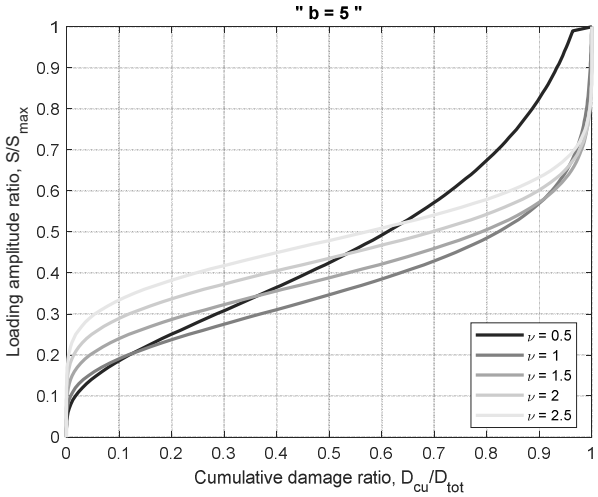

Figure 10: Normalized cumulative damage curves, Heuler's model illustration (b = 5)

Once again, the value "$\nu = 1$" sets the distinction between the different damage spectra shapes. Regarding the "$\nu = 0.5$" curve, the damage cumulative slope is bigger than the other ones. This implies that less damage is provided per amplitude class. It is worth noting that 50% of the overall damage is caused/produced before reaching 40% of the maximum amplitude. The other curves slopes ("$\nu \geq 1$") are quite similar between 10% and 90% of the

overall damage. The main differences between the curves occur before 10% and after 90% of the maximum loading amplitude.

The illustrated damage curves in Figure 10 correspond to a reference Basquin slope ("b = 5"). Accordingly, to the section 2.3, the Figure 11 illustrates the model cumulative damage curve dependence to "b". The higher "b", the less significant in damage calculation are low amplitudes, the more the cumulative damage slope of "ν = 0.5" grows (Figure 11b)). On the contrary, if "b" gets closer down to 2, the cumulative damage slope value of "ν = 0.5" is getting closer to the other slopes as the lowest amplitudes gain impact significance.

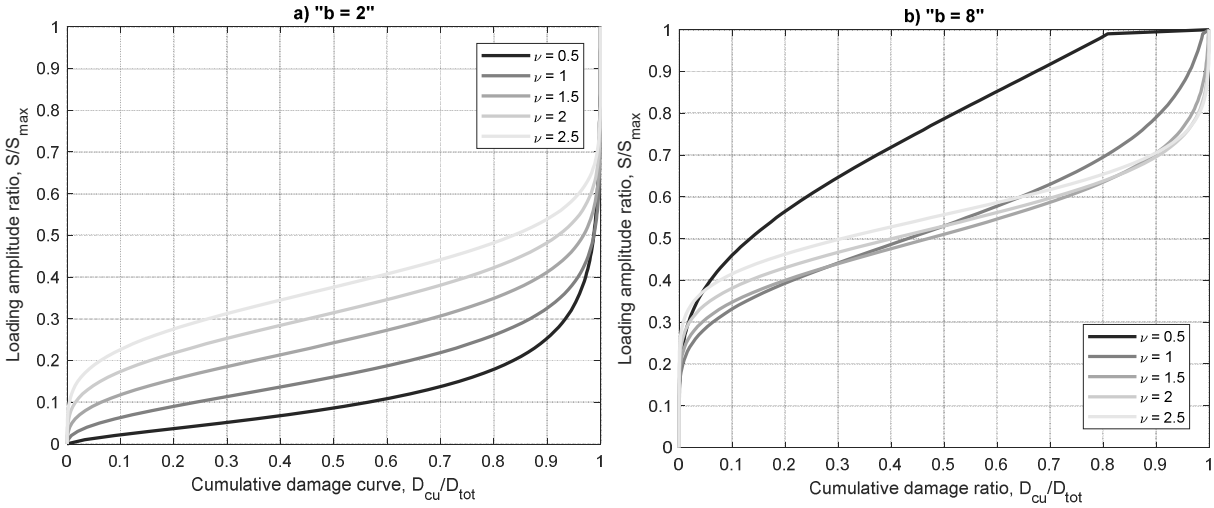

Figure 11: Normalized cumulative damage curves, Heuler's model illustration b = 2 (a), b = 8 (b)

3.2 Model spectrum identification and damage accuracy assessment

As stated previously, Heuler's model is identified on the loading spectrum coming from RLD illustrated in Figure 4. The identification is set in the $(log(H)/\log(H_0) - S/S_{max})$ frame using standard least square identification methods to fit the model to the data. The identified spectrum overall length is fixed to the initial H_0 ($\sim 10^7$) coming from the measurement (Figure 12).

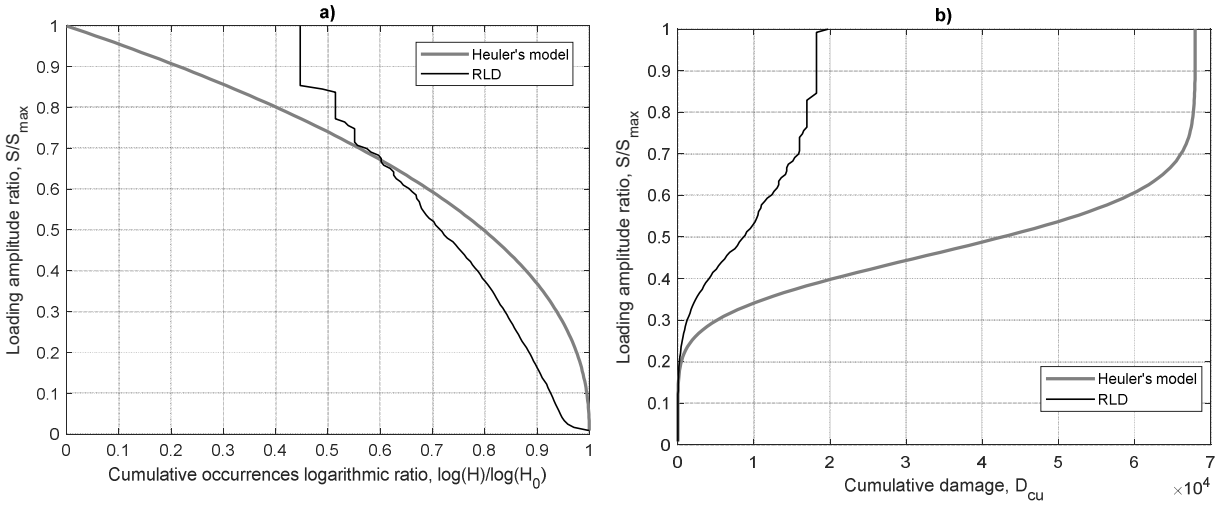

Figure 12: Heuler's model identification on RLD (a), $\boldsymbol{\nu = 2.32}$, and cumulative damage curves (b)

Heuler's model main characteristic is the fixed starting point, no matter the shape factor value, at the coordinates ("$S_1/S_{max} = 1;\ log(H_1)/log(H_0) = 0$"), which means to have one cycle at"S_{max}". In order to fit the loading spectrum, the model tries to catch up this starting level and the following several "steps", from higher amplitudes towards the lower ones.

The comparison graphs (Figure 12b)) of both cumulative damage curves highlights the impact of the amplitude range between 30% and 60% of the maximum amplitude ("*b* = 5": 55% of the RLD damage is made between these two amplitude ratios). Even if there is a slight gap between the two loading curves below "S_i/S_{max} = 0.6", the model inaccuracy gets higher as the frame is a ratio based on logarithmic scale. This identification is not accurate enough as the shape obtained ("$\boldsymbol{\nu = 2.32}$") illustrates a much stiffer behaviour than the initial one. The induced damage is ultimately 3 times bigger than the initial one. Thus, if, experiments were carried out with the identified spectrum instead of the initial RLD, the lifetime would be assessed 3 times shorter, in terms of number of cycles, than the expected one.

The way the RLD spectrum is built (concatenation of several specific manoeuvers) deeply impacts its shape: several cycles are found at the highest amplitudes. This article aims to find a model that may fit in the scope of fatigue design for all the RLD types used by the carmakers. Hence, a model modification must be applied to adapt the spectrum shape specifically at the highest amplitudes and let free the starting loading point value ("$S_1/S_{max} = 1; H_1$").

4 Modified Heuler's model identification

4.1 Model formulation and theoretical investigation

To provide some flexibility considering the depicted behaviours at the highest amplitudes, another parameter, noted "α", is added to the initial Heuler's model. The relationship (9) becomes

$$\log(H)\ /\log(H_0) = 1 - \alpha(S/S_{max})^{\nu}. \qquad \textbf{(10)}$$

Given the model mathematical construction, when "$S_1 = S_{max}$ ", then "$H_1 = H_0^{(1-\alpha)}$", when "H_1" was fixed to 1 with the previous model. Physically, "H_1" is bounded between 1 and "H_0". Hence, "α" is expected between 0 and 1. The previous model corresponds to "$\alpha = 1$.". The Figure 13 illustrates the impact of "α", considering different value of "ν". Once again, the loading spectra are represented using cumulative occurrences and effective cycles, respectively.

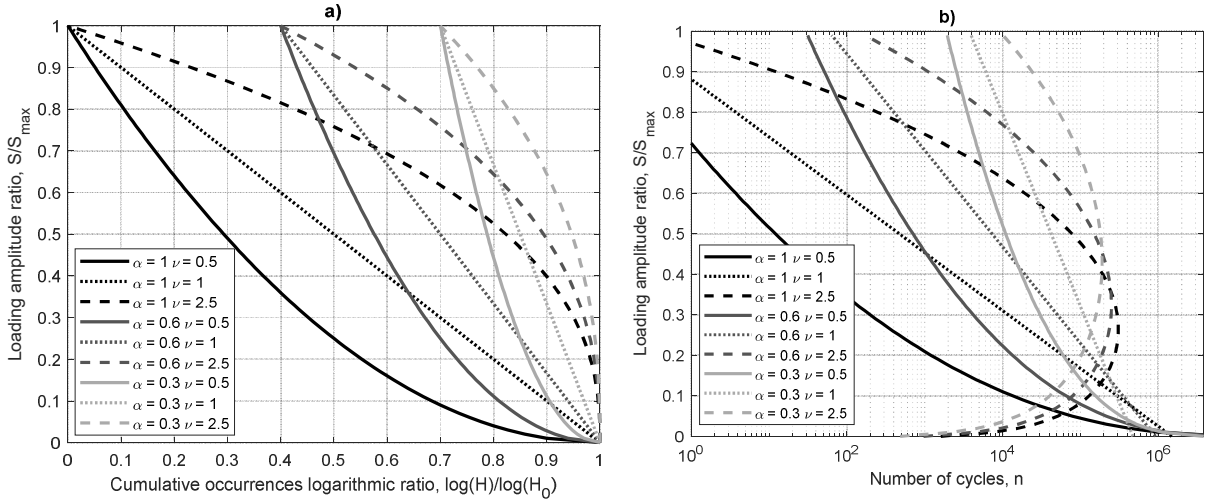

Figure 13: Modified Heuler's model load spectra, via cumulative occurrences (a) and number of cycles (b)

The shape factor "ν" from the initial Heuler's model is kept in this model. Hence, stiff ("$\nu = 2.5$") and smooth ("$\nu = 0.5$") behaviours can still be represented. The "α" parameter influences the loading spectra at the highest amplitudes only. The more "α" decreases, the more the loading curves are shifted to the right. No matter the "α" value, the variety of behaviours at the lowest amplitudes induced by "ν" are quite the same of the initial model curve.

Now that the loading spectra curves are set up, the Figure 14 highlight the cumulative damage caused by these spectra. As the "α" value also affects the overall damage value, only the cumulative damage curves shapes are studied. Each one is respectively normalized by its overall damage induced. Each graph corresponds to one fixed "ν" value and illustrate the impact of "α" on cumulative damage curve shape.

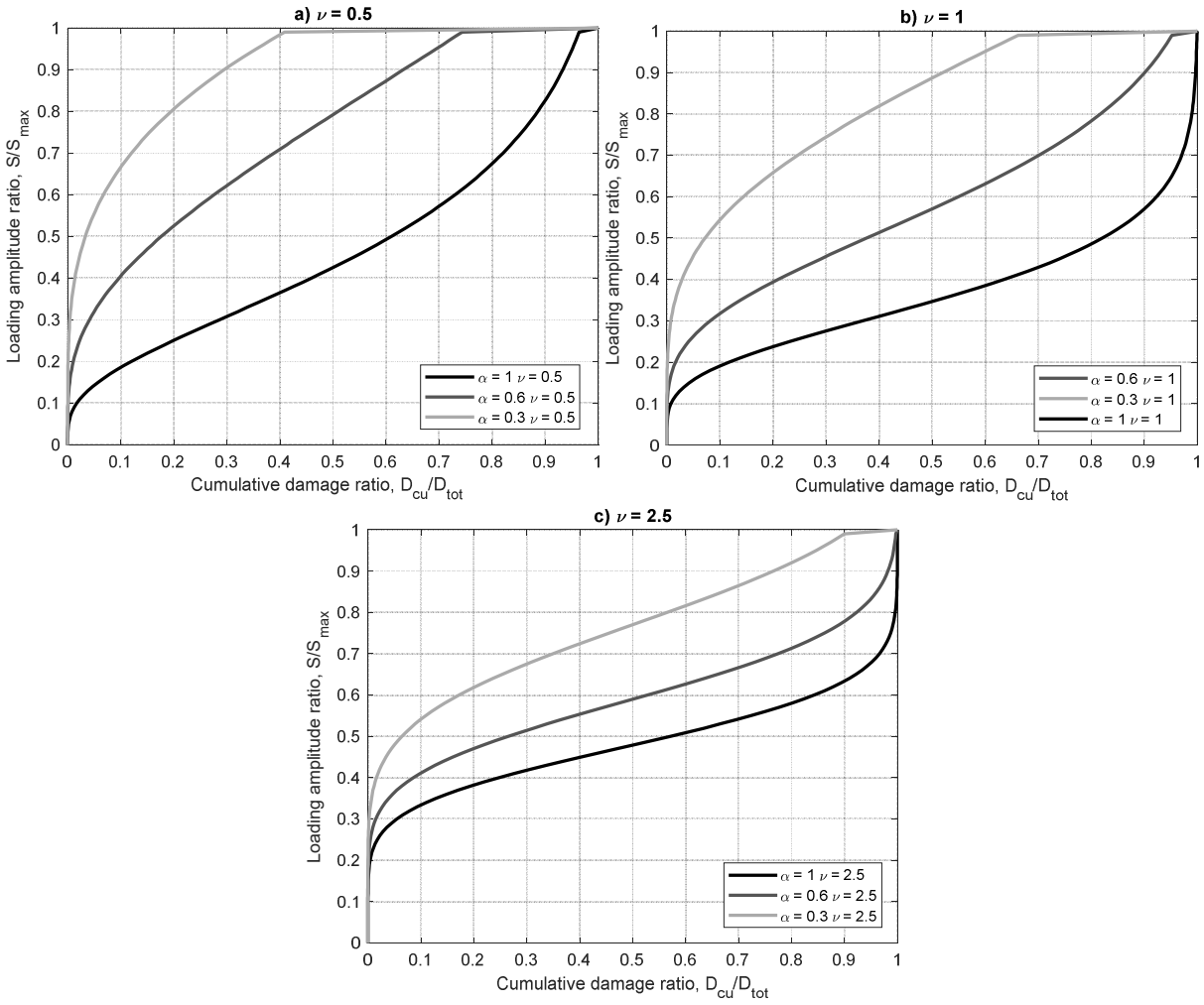

Figure 14: Normalized cumulative damage depending on "α" (b =5), (a)$\nu = 0.5$; (b)$\nu = 1$; (c)$\nu = 2.5$

The more "α" decreases, the more the damage is high amplitudes sensitive. The effect tends to be the same caused by the Basquin slope increase (section 2.3). This is due to the start level reached when "$S_1 = S_{max}$". As "$N_1 = H_1 = H_0^{(1-\alpha)}$", any "$\alpha$" reduction induces a growing shift.

4.2 Model spectrum identification and damage accuracy assessment

In the same way as described in section 3.2, the modified Heuler's model parameters are identified from the RLD. Both "α" and "ν" parameters are left free for the identification. The least squares method is once again applied. The Figure 15 highlights the model identification result.

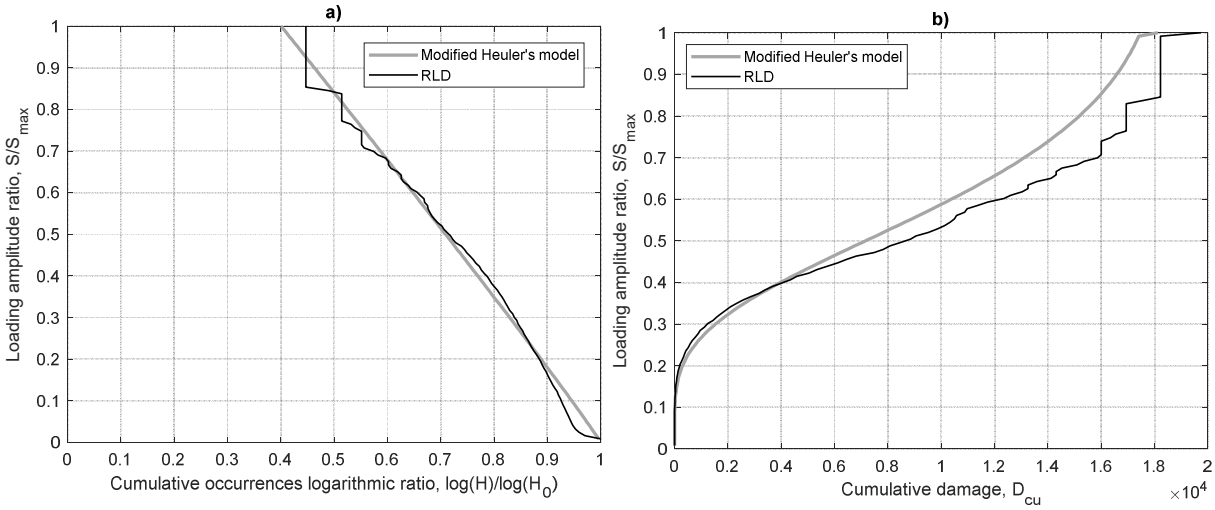

Figure 15: Modified Heuler's model identification on RLD (a), α = 0.59, $\nu = 1.04$, and cumulative damage curves (b)

To consider the starting level at the highest amplitudes, the model set its parameter "α" to 0.59 ("$\log(H_1)/\log(H_0) = 0.4$"). Then, even if there are some visible "steps" on the RLD until the amplitude ratio 0.7, the model is drawn as an almost straight line, ("$\nu = 1.04$") and practically matches the smoother curve part. The behaviour depicted is then less stiff than the one identified with the first model ("$\nu = 2.32$").

Figure 15 b) illustrates the damage cumulative curve caused by the modified model compared to the one coming from the RLD. Comparing both graphs, it is noticeable that the slight shapes difference at the amplitude 0.4 in the loading spectra representation induces the slight cumulative damages curves separation. Still, the overall damage values are quite close ("$D_{cu_{RLD}}/D_{cu_{model}} \sim 0.9$"). Approximately, the same lifetimes are obtained between the two spectra (10% difference on the induced damage indicator). This remains acceptable in terms of lifetime assessment.

Considering both model identifications (Figure 12 and Figure 15), it is noticeable that the modified Heuler's model damaging curve steadily follows the initial one. Even if this model smooths the starting upper "stairs", the lifetime assessment is very close. Thus, the modified Heuler's model fits at least the requirements regarding fatigue design for the specific loading spectra found in the automotive industry.

4.3 Gate implementation

In the section 2.4 a specific tool, named "iso-damaging" curves, has been introduced to detect simultaneously, from the RLD considered, both the most and the less damaging amplitudes. The idea investigated

in this paragraph is to remove from the RLD the least damaging cycles. Then, the modified Heuler's model is once again identified but on the truncated model. The Figure 16 illustrates the Gate implementation on the RLD.

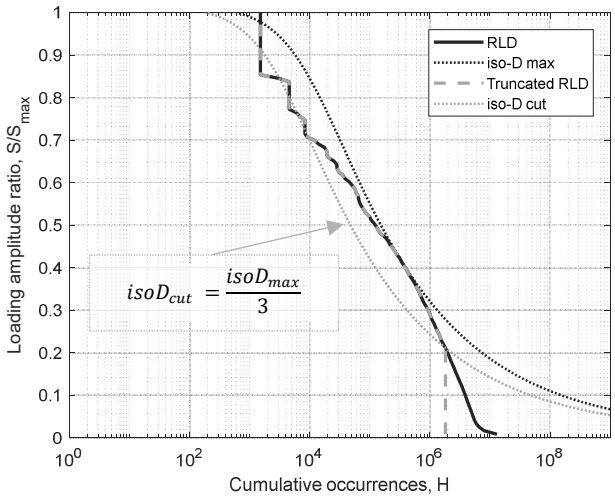

Figure 16: Gate implementation illustration on RLD spectrum

First, the maximum iso-damaging curve is identified between the amplitude ratios "$S_i/S_{max} = 0.7$" and "$S_i/S_{max} = 0.1$". This curve corresponds to the iso-damaging spectrum that induces the most damage and matches the RLD curve in at least one point. The 0.9 limit is set because of the curve stair shape that might bias the identification. The most damaging amplitude corresponds to the amplitude ratio "$S_i/S_{max} = 0.4$".

To implement the gate, the cycles from the RLD that induce less damage than a third of the maximum iso-damaging curve identified can be cut-off from the overall spectrum. This choice is not arbitrary, previous considerations toward this kind of RLD highlight that at least 98% of the overall damage is kept using this cutting off ratio.

The modified Heuler's model is once again identified from the "truncated" RLD. Both parameters are then set to "$\alpha = 0.57$ "and "$\nu = 1.66$" instead of "$\alpha = 0.59$ "and "$\nu = 1.04$" for the overall model. It is tricky to compare both identification as the spectrum overall length has changed due to the gate implementation. Still, as expected, both "α" values are very similar indeed. As illustrated in Figure 17 the gate implementation slightly influences the behavior identified, but not the fatigue lifetime accuracy.

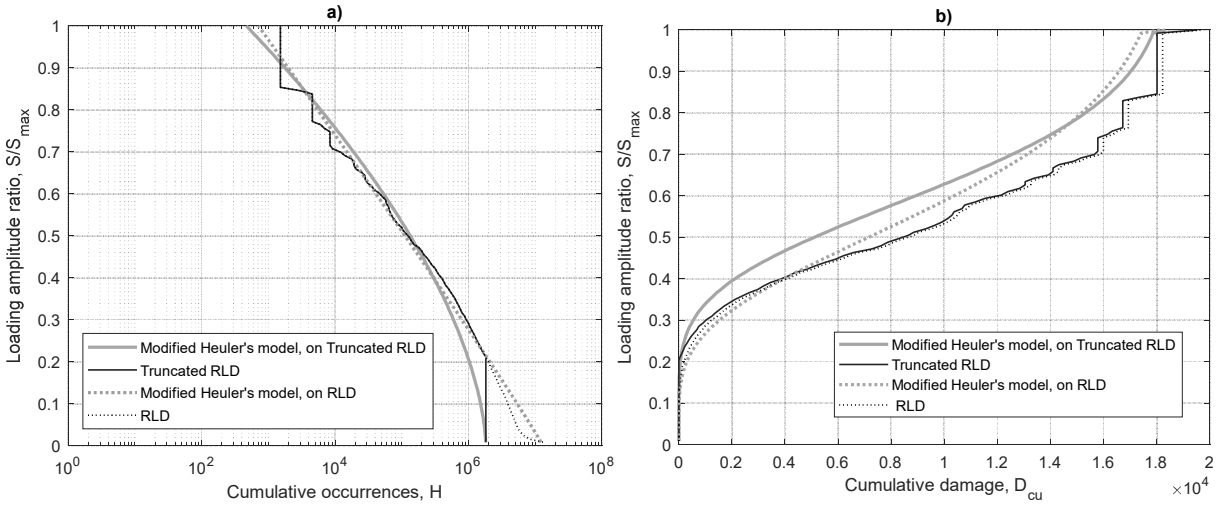

Figure 17: Truncated RLD and model identification ($\alpha = 0.59$), ($\nu = 1.66$), loading spectra (a) and cumulative damage curves (b)

5 Conclusion

This paper highlights a VAL analytical model identification process considering chassis system for high cycle fatigue design. The study is limited to the uniaxial RLD measured directly at the car wheels. These data are basic inputs for the overall chassis system design, no matter of the material, process, technology and geometry diversity of an automotive chassis system.

At first, the spectra analysis using cumulative occurrences representation is shown to offer several advantages. In this framework, an analytical model is proposed and investigated: the modified Heuler's model, inspired by the literature, is based on two parameters whose identification makes effective use of the cumulative representation formulation. To be endorsed, the identified model must cause the same overall damage as the initial RLD, but also corresponds to a certain extent to the damage induced per amplitude range, to keep the strongest physical meaning. The use of cumulative damage curve gathers both information. The model's new "α" parameter enables the identified spectrum to consider a non-unitary cycle spectrum at the highest amplitude. The model's old "ν" parameter keep on transcribing a wide variety of driving behaviours, especially at the lowest amplitudes. Thus, within the fatigue assumptions made the modified Heuler's model is suitable to effectively represent field RLD spectra.

Moreover, further investigations on the damage impact per amplitude class reveals that regardless of how much cycles belong to the lowest amplitudes, they are either not or few damaging. The study of the Basquin slope "b" value significance and the use of "iso-damaging" curves helped to develop an effective gate implementation

methodology. Given an RLD example set with "$b = 5$", 99% of the overall damage induced by the initial spectrum is conserved by removing 87% of the cycles at the lowest amplitudes. And the identified model on the truncated data does not deeply vary from the initial identification.

This study has two main prospects: the development of analytical models designed for the multiaxial framework and the modified Heuler's model identification on standardized spectra coming from other fields (e.g. aeronautics, offshore, …) to compare the spectra shapes and set new standards.

6 Acknowledgements

This work was carried out within the framework of the partnership between Groupe PSA and the OpenLab Computational Mechanics with the financial support of the ANRT for the CIFRE contract n°2019/0764.

7 References

[1] M. L. Facchinetti , C. Doudard, E. Bellec and M. P. Silvestri, "Fatigue Load Spectra: Model and identification proposals for the automotive," *Proceedings of the Fourth International COnference on material and Component Performance under Variable Amplitude Loading (VAL4), scheduled from 30. March to 1. April 2020 in Darmstadt/Germany, DVM, Berlin/Germany,* pp. 201-210, 2020.

[2] C. M. Sonsino, R. Heim and T. Melz, "Why Variable Amplitude Loading ? A Key for Lightweight-Structural Durability Design," in *VAL3, 3rd International Conference on Material and Component Performance under Variable Amplitude Loading*, 2015.

[3] J. Costa, J. Ferreira, L. Borrego et L. Abreu, «Fatigue behaviour of AA6082 friction stir welds under variable loadings,» *International Journal of Fatigue,* vol. 37, pp. 8-16, 2012.

[4] J. Correia, H. Carvalho, G. Lesiuk, A. Mourão, L. Figueiredo Grilo, A. de Jesus et R. Calçada, «Fatigue crack growth modelling of Fão Bridge puddle iron under variable amplitude loading,» *International Journal of Fatigue,* vol. 136, 2020.

[5] S. Vantadori, I. Iturrioz, A. Carpinteri, F. Greco et C. Ronchei, «A novel procedure for damage evaluation of fillet-welded joints,» *International Journal of Fatigue,* vol. 136, 2020.

[6] P. Johannesson and M. Speckert, Guide to load analysis for durability in vehicle engineering, John Wiley & Sons, 2013.

[7] M. Köhler, S. Jenne, K. Pötter and H. Zenner, Load Assumption for Fatigue Design of structures and Components, Springer, 2017.

[8] M. L. Facchinetti, "Fatigue damage of materials and structures assessed by Wöhler and Gassner frameworks: recent insights about load spectra for the automotive," *Procedia Engineering,* vol. 213, pp. 217-225, 2017.

[9] M. L. Facchinetti, "Load Spectra and fatigue damage: applications to the automotive industry," *MATEC Web Conferences,* vol. 165, no. 17008, 2018.

[10] P. Heuler and H. Klätschke, "Generation and use of standardised load spectra and load-time histories," *International Journal of Fatigue,* vol. 27, pp. 974-990, 2005.

[11] P. Heuler, T. Bruder and H. Klätschke, "Standardised load-time histories - A contribution to durability issues under spectrum loading," *Materialwissenschaft und Werkstofftechnik,* vol. 36, pp. 669-677, 2005.

[12] C. M. Sonsino, «Fatigue testing under variable amplitude loading,» *International Journal of Fatigue,* vol. 29, pp. 1080-1089, 2007.

[13] C. Berger and al., "Betriebsfestigkeit in Germany - an overview," *International Journal of Fatigue,* vol. 24, pp. 603-625, 2002.

[14] V. Grubisic, «Determination of load spectra for design and testing,» *International Journal of Vehicle Design,* vol. 15, 1994.

[15] R. Heim, G. Fischer and C. M. Sonsino, "Early stage rig testing durability approval," *SAE Technical paper,* no. 2006-01-0116, 2006.

[16] T. Voigt, K. Lipp and T. Melz, "Fatigue strength assessment for components and subsystems of a lightweight, space saving city car with electric drive," *Procedia Structural integrity,* vol. 19, pp. 4-11, 2019.

[17] C. Bathias and J. P. Baïlon, La Fatigue des matériaux et des structures - Fatigue of materials and structures, Hermès Paris, 1997 (in French).

[18] S. Suresh, Fatigue of Materials, Cambridge Solid State Science Series, 1998.

[19] I. Raoult and B. Delattre, "Fatigue equivalent load approach for fatigue design of uncertain structures," *Proceedings of the 12th International Conference on Multiaxial Fatigue and Fracture (Bordeaux, 2019), MATEC Web of Conferences,* vol. 300, no. 02003, 2019.

[20] D. Schütz, H. Klätschke, H. Steinhilber, P. Heuler and W. Schütz, "Standardized load sequences for car wheel suspension components, Car Loading Standard - CARLOS," *Fraunhofer-Institut für Beriebsfestigkeit (LBF) Report,* no. 191, 1999.

[21] D. Schütz, H. Klätschke and P. Heuler, "Standardized multiaxial load sequences for car wheel suspension components - Car Loading Standards - CARLOS multi," *Fraunhofer-Insitut für Betriebsfeistigkeit (LBF), Report,* no. 201, 1994.

[22] E. Haibach, R. Fischer, W. Schütz et M. Hück, «A standard random load sequence of Gaussian type recommended for general application in fatigue testing; its mathematical background and digital generation,» *Fatigue testing and Design : Papers presented at the international Conference 5-9th April 1976, at the City University, London,* pp. 29.1-29.21, 1976.

[23] D. Schütz, H. Lowak, J. B. De Jonge and J. Schijve, "A standardised load sequence for flight simulation tests on transport aircraft winf structures," *Fraunhofer-Institut für Betriebsfestigkeit (LDF),* no. Report FB-106, NLR- Report 73, 1973.

[24] M. Brune and H. Zenner, "Verbesserung der Lebensdauerabschätzung für Bauteile in Walwerksantrieben (Improvement of life prediction for components of steel mill drives).," *VBFEh Report,* no. ABF40.1, 1990.

[25] O. H. Basquin, «The exponential law of endurance tests,» *Proceedings of the ASTM,* vol. 10, pp. 625-630, 1919.

[26] A. Wöhler, «Versuche zur Ermittlung der auf die Eisenbahnwagenachsen einwirkenden Kräfte und die Widerstandsfähigkeit des Wagen-Achsen,» *Zeitschrift für Bauwesen,* vol. 10, pp. 583-616, 1860 (in German).

[27] S. Bergamo, P. Schimmerling, F. Triboulet, P. Wilson, M. L. Facchinetti, M. Monin, F. Lefebvre and B. Weber, "Préconisations pour les caractéristiques statistiques de résistance en fatigue - Applications aux aciers et autres matériaux utilisés dans la construction automobiles," *SIA ,* 2017 (in French).

[28] E. Gassner, «Festigkeitsversuche mit wiederholter Beanspruchung im Flugzeugbau - Strength tests under repeated loading for aeronautical engineering,» *Luftwissen ,* vol. 6, pp. 61-64, 1939 (in German).

[29] A. Palmgren, «Die Lebensdauer von Kugellagern - The Fatigue Life of Ball-Bearings,» *Zeitschrift des vereins Deutscher Ingenieure,* vol. 68, pp. 339-341, 1924 (In German).

[30] M. A. Miner, "Cumulative damage in fatigue," *Journal of Applied Mechanics,* vol. 12, pp. A159-A164, 1945.